

Electron and Hole Spin Splitting and Photogalvanic Effect in Quantum Wells

L.E. Golub*

A.F. Ioffe Physico-Technical Institute, Russian Academy of Sciences, 194021 St. Petersburg, Russia

A theory of the circular photogalvanic effect caused by spin splitting in quantum wells is developed. Direct interband transitions between the hole and electron size-quantized subbands are considered. It is shown that the photocurrent value and direction depend strongly on the form of the spin-orbit interaction. The currents induced by structure-, bulk-, and interface-inversion asymmetry are investigated. The photocurrent excitation spectra caused by spin splittings in both conduction and valence bands are calculated.

PACS numbers: 72.40.+w, 72.20.My, 72.25.Rb, 72.25.-b, 73.63.Hs

I. INTRODUCTION

The spin properties of carriers have attracted much attention in recent years due to rapidly developed spintronics dealing with the manipulation of spin in electronic devices.¹ The first idea was put forward by Datta and Das, who proposed a spin field-effect transistor.² Its work is based on a change of the Rashba field in semiconductor heterostructures, caused by structure inversion asymmetry (SIA).³

The promising materials for spintronics are III-V semiconductor quantum wells (QWs) whose spin properties are well documented and can be controlled by advanced technology. However, in addition to the Rashba spin-orbit interaction, other effective magnetic fields act on carriers in zinc-blende heterostructures. This is, first, the so-called Dresselhaus field caused by bulk inversion asymmetry (BIA).^{4,5,6,7,8,9} It is present in QWs made of semiconductors without inversion center.

Second, there is the spin-orbit interaction produced by the interface inversion asymmetry (IIA). It has been established that the single-interface symmetry allows heavy-light hole mixing at zero in-plane wave vector.^{10,11,12,13,14,15,16,17} This mixing gives rise to spin splitting in both valence and conduction bands at nonzero wave vector.^{18,19,20,21} The structure of the corresponding linear in the wave vector contribution to the electron effective Hamiltonian coincides with that due to BIA.²¹ In the following both contributions, BIA and IIA, are considered together as a generalized BIA field.

Both SIA and BIA give rise to many spin-dependent phenomena in QWs, such as an existence of beats in the Shubnikov-de Haas oscillations,²² spin relaxation,⁴ splitting in polarized Raman scattering spectra,²³ and positive anomalous magnetoresistance.²⁴ Spin splittings and relaxation times have been extracted from these experiments. However, in (001)-grown QWs, the SIA and BIA spin-orbit interactions result in the same dependences of spin splittings and spin relaxation times on the wave vector. Therefore it is impossible to determine the nature for the spin splitting at low wave vectors. Only in the simultaneous presence of both BIA and SIA of comparable strengths, one can observe new effects, see Ref. 25 and references therein. However the latter situation is rare

in real systems because it requires a special structure design. Usually SIA and BIA cannot be distinguished in experiments.

In this work, the other spin-dependent phenomenon is investigated which is essentially different from the ones mentioned above. This is the *Circular Photo-Galvanic Effect* which is a conversion of photon angular momentum into a directed motion of charge carriers. The result is an appearance of electric current under absorption of a circularly-polarized light.²⁶ The photocurrent reverses its direction under inversion of the light helicity. Microscopically, the circular photocurrent appears owing to a coupling between orbital and spin degrees of freedom. In semiconductors the coupling is a consequence of the spin-orbit interaction. In two-dimensional systems, the circular photogalvanic effect can be caused by both Rashba and Dresselhaus effective magnetic fields. In this paper we show that SIA and BIA result in experimentally distinguishable photocurrents.

The recently started activity on circular photogalvanics in QWs attracted much attention.^{27,28} The photocurrents induced by both SIA and BIA have been investigated. The circular photocurrent has been mostly studied under *intra*band transitions induced by infrared or far-infrared excitations. However it is important to extend studies on the optical range where the effect is expected to be much stronger. In this case, the photocurrent appears due to *inter*band transitions.

In the present work, the theory of the interband circular photogalvanic effect in QWs is developed, and the photocurrent spectra are calculated.

II. GENERAL THEORY

In the absence of a spin-orbit interaction, two states with the same wave vector \mathbf{k} in the same size-quantized subband, $|1\rangle$ and $|2\rangle$, are degenerate. In a symmetrical QW, the electron envelope functions of these states can be chosen in the form

$$|1_e\rangle = \exp(i\mathbf{k}\cdot\boldsymbol{\rho})\varphi(z)\uparrow, |2_e\rangle = \exp(i\mathbf{k}\cdot\boldsymbol{\rho})\varphi(z)\downarrow, \quad (1)$$

where z is the growth direction, $\boldsymbol{\rho}$ is the electron position in the plane of QW, and \uparrow and \downarrow are the spin-up and

spin-down functions. For odd (even) subbands of size-quantization, $\varphi(-z) = \pm\varphi(z)$, respectively.

The two degenerate hole states with the wave vector \mathbf{k} can be chosen as symmetrical and antisymmetrical with respect to the mirror reflection in the plane located in the middle of the QW. The wave function for the symmetrical state has the form²⁹

$$\begin{aligned} |1_h\rangle &= \exp(i\mathbf{k}\cdot\rho) \\ &\times N \left\{ - \left[u_{3/2} + \sqrt{3}W_+ \exp(2i\phi_{\mathbf{k}})u_{-1/2} \right] \chi_+(z) \right. \\ &\left. + i \left[\exp(3i\phi_{\mathbf{k}})u_{-3/2} + \sqrt{3}W_- \exp(i\phi_{\mathbf{k}})u_{1/2} \right] \chi_-(z) \right\}, \end{aligned} \quad (2)$$

and the antisymmetrical wave function $|2_h\rangle$ can be obtained from $|1_h\rangle$ by applying the operations of time and space inversion. Here $u_{\pm 3/2}$, $u_{\pm 1/2}$ are the Bloch functions at the top of the valence band, χ_+ and χ_- are, respectively, even and odd functions of coordinate z ,³⁰ and $\phi_{\mathbf{k}}$ is the angle between $[100]$ and \mathbf{k} :

$$\tan \phi_{\mathbf{k}} = k_y/k_x.$$

Spin-orbit interaction in QWs is described by the Hamiltonian which has the following form in the basis of two states $|1\rangle$ and $|2\rangle$

$$H(\mathbf{k}) = \boldsymbol{\sigma} \cdot \boldsymbol{\Omega}(\mathbf{k}). \quad (3)$$

Here σ_x, σ_y are the Pauli matrices acting on the states $|1\rangle$ and $|2\rangle$. The effective \mathbf{k} -dependent magnetic field $\mathbf{B}_{eff} \propto \boldsymbol{\Omega}(\mathbf{k})$ is determined by the type of inversion asymmetry.

In the presence of the spin-orbit interaction (3), the two eigenstates with a given wave vector \mathbf{k} are split by $\Delta = 2|\boldsymbol{\Omega}(\mathbf{k})|$. We denote these states by the index $m = \pm$. Their envelope functions in size-quantized subbands can be chosen in the form

$$|m\rangle = \frac{m}{\sqrt{2}} \exp(-i\Phi_{\mathbf{k}}) |1\rangle + \frac{1}{\sqrt{2}} |2\rangle, \quad (4)$$

where the phase $\Phi_{\mathbf{k}}$ is given by

$$\tan \Phi_{\mathbf{k}} = \Omega_y/\Omega_x.$$

Let us now consider optical excitation of a QW by circularly-polarized light (see Fig. 1). Here we investigate the photocurrent arising due to asymmetry of the carrier distribution in the \mathbf{k} -space at the moment of creation. It is different from another photocurrent caused by carrier momentum redistribution during the process of spin relaxation. The latter, so-called spin-galvanic effect, was considered in Refs. 31 and 28. These two photocurrents can be separated in the time-resolved experiments: after switching-off the light source, the former decays with the momentum relaxation time while the latter disappears within the spin relaxation time.

The electric current is expressed in terms of the velocity operators and spin density matrices for electrons and holes as follows

$$\mathbf{j} = e \sum_{\mathbf{k}} \text{Tr} \left[\mathbf{v}^{(e)}(\mathbf{k}) \rho^{(e)}(\mathbf{k}) - \mathbf{v}^{(h)}(\mathbf{k}) \rho^{(h)}(\mathbf{k}) \right], \quad (5)$$

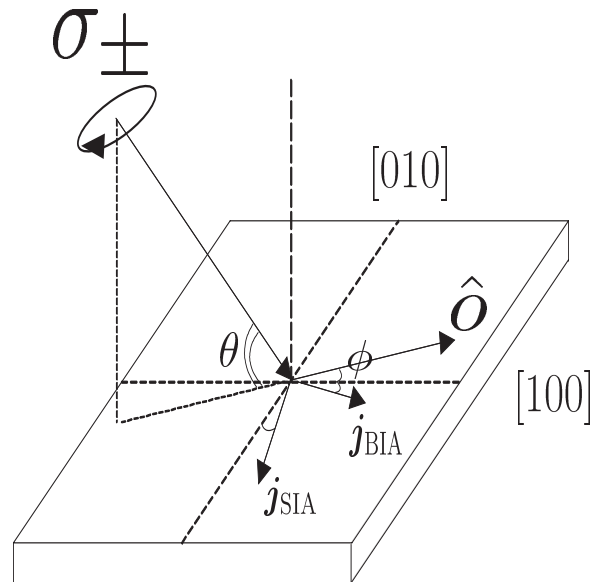


FIG. 1: SIA- and BIA-induced photocurrents appearing under oblique incidence of circularly-polarized light.

where e is the electron charge.

Density-matrix equations taking into account both direct optical transitions and elastic scattering give the following expressions for linear in the light intensity values entering into Eq.(5)

$$\begin{aligned} \rho_{nn'}^{(e,h)} &= \pm \frac{\pi}{\hbar} \tau_{e,h} \sum_{\bar{n}} M_{n\bar{n}} M_{\bar{n}n'} \left[\delta(E_n + E_{\bar{n}} - \hbar\omega) \right. \\ &\quad \left. + \delta(E_{n'} + E_{\bar{n}} - \hbar\omega) \right]. \end{aligned} \quad (6)$$

Here τ_e and τ_h are the relaxation times of electrons and holes (here we assume isotropic scattering), $\hbar\omega$ is the photon energy, $M_{n\bar{n}}(\mathbf{k})$ is the matrix element of the direct optical transition between the states n and \bar{n} , and the energy dispersions $E_{e,h}(\mathbf{k})$ are reckoned inside the bands.

Spin splittings of electron or hole subbands both give rise to the circular photogalvanic effect. The corresponding contributions to the current are independent, therefore we consider the cases of electron and hole spin splittings separately.

III. ELECTRON SPIN-SPLITTING INDUCED PHOTOCURRENT

Here we take into account spin splitting in the conduction band. In QWs, the spin-orbit interaction Eq. (3) is described by the linear in the wave vector Hamiltonian

$$\Omega_i(\mathbf{k}) = \beta_{il} k_l. \quad (7)$$

Cubic in \mathbf{k} corrections do not result in a circular photogalvanic effect, therefore we do not consider them below.

Tensor β is determined by the symmetry of the QW. As mentioned in the Introduction, in structures with a zinc-blende lattice, there is a contribution due to BIA and IIA

known as the Dresselhaus term. For (001)-grown QWs, it has two non-zero components, namely

$$\beta_{xx} = -\beta_{yy} \equiv \beta_{\text{BIA}}, \quad (8)$$

where $x \parallel [100]$ and $y \parallel [010]$.

SIA appears due to difference of the right and left barrier heights of the QW, electric fields applied along z direction, etc. It leads to an additional contribution to the spin-orbit Hamiltonian, the so-called Rashba term:

$$\beta_{xy} = -\beta_{yx} \equiv \beta_{\text{SIA}}. \quad (9)$$

The velocity matrix elements calculated on the wave functions (4) taking into account the spin-orbit corrections (3), are given by

$$\begin{aligned} \left(v_i^{(e)} \right)_{mm'} &= \left[\frac{\hbar k_i}{m_e} + \frac{m}{\hbar} (\beta_{xi} \cos \Phi_{\mathbf{k}} + \beta_{yi} \sin \Phi_{\mathbf{k}}) \right] \delta_{mm'} \\ &+ \frac{im}{\hbar} (\beta_{yi} \cos \Phi_{\mathbf{k}} - \beta_{xi} \sin \Phi_{\mathbf{k}}) (1 - \delta_{mm'}), \\ v_i^{(h)} &= \frac{k_i}{k} v_h(k), \quad v_h(k) = \frac{1}{\hbar} \frac{dE_h(k)}{dk}, \end{aligned} \quad (10)$$

where m_e is the electron effective mass.

Calculations show that all odd Fourier harmonics of $\rho^{(e,h)}(\mathbf{k})$ entering into (5) are proportional to the following part of the sum

$$\begin{aligned} \sum_{l=\{1_h\}, \{2_h\}} M_{ml} M_{lm'} &\propto P_{\text{circ}} \left(\frac{epA_0}{m_0 c} \right)^2 \sin \theta (NQ_{\pm})^2 m \\ &\times \{ \delta_{mm'} [W_{\pm} \cos(\Phi_{\mathbf{k}} - 2\phi_{\mathbf{k}} + \phi) + W_{\pm}^2 \cos(\Phi_{\mathbf{k}} - \phi)] \\ &+ i(1 - \delta_{mm'}) \\ &\times [W_{\pm} \sin(\Phi_{\mathbf{k}} - 2\phi_{\mathbf{k}} + \phi) + W_{\pm}^2 \sin(\Phi_{\mathbf{k}} - \phi)] \}. \end{aligned} \quad (11)$$

Here P_{circ} is the circular polarization degree, θ and ϕ are the spherical angles of the light polarization vector (see Fig. 1), p is the interband momentum matrix element, A_0 is the light wave amplitude, m_0 is the free electron mass, and

$$Q_{\pm} = \int_{-\infty}^{\infty} dz \varphi(z) \chi_{\pm}(z). \quad (12)$$

The upper (lower) sign in Eq. (11) corresponds to excitation into the odd (even) electron subbands.³⁰

The characteristic spin splittings are usually very small, therefore we consider a linear in β regime. In this approximation, SIA and BIA give independent contributions into the photocurrent

$$\mathbf{j}(\omega) = \mathbf{j}_{\text{SIA}}(\omega) + \mathbf{j}_{\text{BIA}}(\omega), \quad (13)$$

where \mathbf{j}_{SIA} and \mathbf{j}_{BIA} are linear in β_{SIA} and β_{BIA} , respectively. Assuming the splitting $\Delta \rightarrow 0$ and calculating the reduced density of states, we obtain from Eqs. (5) - (12) the expressions for the interband circular photocurrents:

$$j_i(\omega) = -\beta_{li} \hat{o}_l P_{\text{circ}} \left(\frac{epA_0}{m_0 \hbar c} \right)^2 \frac{e}{\hbar} G(k_{\omega}). \quad (14)$$

Here $i, l = x, y$, and \hat{o} is a projection of the unit vector along the light propagation direction on the QW plane (see Fig. 1). The wave vector of the direct optical transition, k_{ω} , satisfies the energy conservation law

$$E_e(k_{\omega}) + E_h(k_{\omega}) = \hbar\omega - E_g, \quad (15)$$

where $E_e(k) = \hbar^2 k^2 / 2m_e$ is the electron energy without spin-orbit corrections, and $E_h(k)$ stands for the hole dispersion, calculated in the spherical approximation.

We study the effects linear in β , therefore Eq. (14) is valid at $\hbar\omega - E_g^{QW} \gg \beta k_{\omega}$, where $E_g^{QW} = E_g + E_{e1}(0) + E_{h1}(0)$ is the fundamental energy gap corrected for the energies of size-quantization. However for real systems, the theory is valid even near the absorption edge.

The frequency dependence of the photocurrent is given by the function $G(k)$

$$G(k) = \frac{k}{v(k)} \frac{d}{dk} \left[\frac{F(k)u(k)}{v(k)} \right] + \frac{F(k)}{v(k)} \left[\frac{u(k)}{v(k)} - 2 \right], \quad (16)$$

where

$$\begin{aligned} F(k) &= k [N(k)Q_{\pm}(k)W_{\pm}(k)]^2 \tau_e(k), \\ v(k) &= \frac{\hbar k}{m_e} + v_h(k), \quad u(k) = \left[\frac{\hbar k}{m_e} + v_h(k) \frac{\tau_h(k)}{\tau_e(k)} \right] \xi(k). \end{aligned} \quad (17)$$

The first term in Eq. (16) appears because the direct transitions to the upper (lower) spin branch take place at a wave vector slightly smaller (larger) than k_{ω} , and the second term occurs because the two electron spin states with the same \mathbf{k} have different velocities.

The factor $\xi(k)$ depends on the form of a spin-orbit interaction. It follows from Eqs. (8), (9) that, for the BIA-induced spin-orbit interaction, $\Phi_{\mathbf{k}} = -\phi_{\mathbf{k}}$, while, for SIA-dominance, $\Phi_{\mathbf{k}} = \phi_{\mathbf{k}} - \pi/2$. Therefore one has

$$\xi_{\text{BIA}} = 1, \quad \xi_{\text{SIA}} = 1 - 1/W_{\pm}(k). \quad (18)$$

The difference appears because in the BIA-case the terms with W_{\pm} in Eq. (11) are the third harmonics of $\phi_{\mathbf{k}}$ and, hence, do not contribute to the current. This means that BIA and SIA create different current distributions of optically-generated electrons.

This difference gives rise to non-equal frequency dependences of the photocurrent. It is dramatic at the absorption edge, when $\hbar\omega \geq E_g^{QW}$. For the ground hole subband $W_{+}(k) \sim k^2$, and hence

$$j_{\text{BIA}} \sim (\hbar\omega - E_g^{QW})^2, \quad j_{\text{SIA}} \sim \hbar\omega - E_g^{QW}. \quad (19)$$

This conclusion opens a possibility to distinguish experimentally which kind of asymmetry, BIA or SIA, is dominant in the structure under study. This could be done by studying the power, quadratic or linear, in the dependence of the circular photocurrent on the light frequency near the absorption edge. At higher photon energies, the spectra are also different due to k -dependence of the functions W_{\pm} [see Eq. (18)].

IV. HOLE SPIN-SPLITTING INDUCED PHOTOCURRENT

In this section we calculate the circular photocurrent which arises due to the spin splitting in the valence size-quantized subbands. The split hole states have wave functions Eq. (4), the two degenerate states in the conduction band are given by Eq. (1).

SIA and BIA result in the hole spin splitting as well as for electrons. Below we consider both cases and derive the expressions for circular photocurrents.

A. SIA-induced circular photocurrent

SIA is described by the hole Hamiltonian^{32,33} which has the following form in the basis $u_{3/2}$, $u_{1/2}$, $u_{-1/2}$, $u_{-3/2}$

$$H(\mathbf{k}) = -i\alpha k \begin{pmatrix} 0 & 0 & 0 & 0 \\ 0 & 0 & e^{-i\phi_{\mathbf{k}}} & 0 \\ 0 & -e^{i\phi_{\mathbf{k}}} & 0 & 0 \\ 0 & 0 & 0 & 0 \end{pmatrix}. \quad (20)$$

In a weak electric field applied along the growth direction, the k -independent coefficient α is proportional to its strength.

In the basis $|1_h\rangle$, $|2_h\rangle$ the Hamiltonian Eq. (20) has the form of Eq. (3) with

$$\Omega_x + i\Omega_y = \langle 2_h | H | 1_h \rangle = iA \exp(3i\phi_{\mathbf{k}}), \quad (21)$$

where

$$A = 3\alpha k N^2 \left(W_+^2 \int_{-\infty}^{\infty} dz \chi_+^2(z) + W_-^2 \int_{-\infty}^{\infty} dz \chi_-^2(z) \right). \quad (22)$$

The splitting equals to $\Delta = 2|A(k)|$, and the phase $\Phi_{\mathbf{k}} = 3\phi_{\mathbf{k}} + \pi/2$.

At $k \rightarrow 0$, for the $h1$ subband one has $\Delta \sim k^3$. For the $l1$ subband, the Hamiltonian in the basis $\exp(2i\phi_{\mathbf{k}})|2_h\rangle$, $\exp(-2i\phi_{\mathbf{k}})|1_h\rangle$ has the form

$$H(\mathbf{k}) = \alpha(\sigma_x k_y - \sigma_y k_x),$$

i.e. it is similar to the SIA-Hamiltonian for electrons, Eqs. (7), (9). The splitting in this case is linear in k . In real experiments, the hole wave vector may be large, therefore we take into account the nonparabolicity effects and allow explicit k -dependence $A(k)$ in Eq. (21).

Calculating the photocurrent, we arrive at the expression (14) with the k -dependent tensor β given by

$$\beta_{xy}(k) = -\beta_{yx}(k) = \frac{dA}{dk} \quad (23)$$

and with the following function $G(k)$ which determine the photocurrent excitation spectrum

$$G(k) = \frac{k}{\gamma(k)v(k)} \frac{d}{dk} \left[\frac{F(k)u(k)}{v(k)} \right] + \frac{F(k)}{v(k)} \left[\frac{u(k)}{v(k)} - 2 + \left(1 + \frac{1}{W_{\pm}(k)} \right) \left(1 \pm \frac{3}{\gamma(k)} \right) \right]. \quad (24)$$

Here F , u and v are given by Eq. (17) with $\xi = 1 - 1/W_{\pm}$ and interchange $\tau_e \leftrightarrow \tau_h$. The factor γ

$$\gamma(k) = \frac{d \ln A}{d \ln k}. \quad (25)$$

At $k \rightarrow 0$, $\gamma = 3$ for the $h1$ -subband and $\gamma = 1$ for the $l1$ -subband. The edge behavior of the spectrum is governed by the $h1 \rightarrow e1$ transitions and follows the quadratic law

$$j_{\text{SIA}} \sim (\hbar\omega - E_g^{QW})^2. \quad (26)$$

B. BIA- and IIA-induced circular photocurrent

IIA is described by the interface term in the Hamiltonian^{11,12,13,33,34}

$$H_{\text{IIA}} = \frac{\hbar^2}{m_0 a_0 \sqrt{3}} t_{l-h}^{(i)} \{J_x, J_y\} \delta(z - z_i). \quad (27)$$

Here z_i are coordinates of the left ($i = L$) and the right ($i = R$) interfaces, a_0 is the lattice constant, and $J_{x,y}$ are the operators of angular momentum $3/2$. The heavy-light hole mixing coefficients at two interfaces of A_3B_5 QWs are related by

$$t_{l-h}^{(L)} = -t_{l-h}^{(R)}.$$

The BIA-contribution for holes in the bulk is described by the Hamiltonian:^{26,35}

$$H_{\text{BIA}} = \frac{4}{3} c_1 \mathbf{K} \cdot \mathbf{V} + c_3 [J_x K_x (K_y^2 - K_z^2) + J_y K_y (K_z^2 - K_x^2) + J_z K_z (K_x^2 - K_y^2)]. \quad (28)$$

Here c_1 and c_3 are the relativistically-small and non-relativistic valence-band spin-orbit constants, respectively, $\mathbf{K} = (\mathbf{k}, -id/dz)$ is the three-dimensional wave vector, and $V_x = \{J_x, (J_y^2 - J_z^2)\}$ etc. In Eq. (28) we neglected the cubic in K relativistically-small terms.

In the basis $|1_h\rangle$, $|2_h\rangle$ both Hamiltonians (27) and (28) have the form of Eq. (3) with

$$\Omega_x + i\Omega_y = B_1 \exp(5i\phi_{\mathbf{k}}) + B_2 \exp(i\phi_{\mathbf{k}}), \quad (29)$$

where

$$B_{1,2} = \pm 3N^2 \left\{ \frac{2\hbar^2}{\sqrt{3}m_0 a_0} W_{\pm} t_{l-h}^{(i)} \chi_{+}(z_i) \chi_{-}(z_i) + c_3 k \left[W_{\pm}^2 \int_{-\infty}^{\infty} dz (d\chi_{\pm}/dz)^2 - W_{\mp} \int_{-\infty}^{\infty} dz (d\chi_{\mp}/dz)^2 \right] \right\} \quad (30)$$

$$\begin{aligned}
& + \left[c_3 \frac{k^3}{4} (1 - W_{\pm}) - c_1 k \right] W_{\pm}^2 \int_{-\infty}^{\infty} dz \chi_{\pm}^2(z) \\
& + \left[c_3 \frac{k^3}{4} (1 - W_{\mp}) - c_1 k \frac{1 + 2W_{\mp}}{3} \right] \int_{-\infty}^{\infty} dz \chi_{\mp}^2(z) \Big\}.
\end{aligned}$$

The splitting is given by

$$\Delta = 2\sqrt{B_1^2 + B_2^2 + 2B_1B_2 \cos 4\phi_k}.$$

It is seen from Eq. (30) that IIA and BIA give additive contributions to the spin-orbit interaction: the coefficients $B_{1,2}$ have the terms proportional to $t_{l-h}^{(i)}$ and to $c_{1,3}$. At $k \rightarrow 0$ for the $h1$ subband $B_1 \sim k^5$, $B_2 \sim k$.

Calculating the photocurrent, we arrive at the expression

$$\begin{aligned}
j_i(\omega) &= -P_{\text{circ}} \frac{e}{\hbar} \left(\frac{epA_0}{m_0\hbar c} \right)^2 \\
&\times \left[\beta_{li}^{(1)}(k_\omega) G_1(k_\omega) + \beta_{li}^{(2)}(k_\omega) G_2(k_\omega) \right] \hat{o}_l.
\end{aligned} \quad (31)$$

The k -dependent tensors β are given by

$$\beta_{xx}^{(1,2)}(k) = -\beta_{yy}^{(1,2)}(k) = \frac{dB_{1,2}}{dk} \quad (32)$$

and

$$\begin{aligned}
G_{1,2}(k) &= \frac{k}{\gamma_{1,2}(k)v(k)} \frac{d}{dk} \left[\frac{F_{1,2}(k)u(k)}{v(k)} \right] \\
&+ \frac{F_{1,2}(k)}{v(k)} \left[\frac{u(k)}{v(k)} - 1 + \nu_{1,2}(k) \right].
\end{aligned} \quad (33)$$

Here u and v are defined by Eq. (17) with $\xi = 1$ and interchange $\tau_e \leftrightarrow \tau_h$; $\gamma_{1,2} = d \ln B_{1,2} / d \ln k$,

$$\nu_1(k) = -5/\gamma_1(k), \quad \nu_2(k) = 1/\gamma_2(k), \quad (34)$$

$$\begin{aligned}
F_1 &= \pm k (NQ_{\pm})^2 \tau_h W_{\pm}^{3/2 \pm 1/2}, \\
F_2 &= \pm k (NQ_{\pm})^2 \tau_h W_{\mp}^{3/2 \mp 1/2}.
\end{aligned} \quad (35)$$

The upper (lower) sign should be taken for transitions to the odd (even) electron subbands.

At the absorption edge we have the linear law

$$j_{\text{BIA}} \sim \hbar\omega - E_g^{\text{QW}}. \quad (36)$$

The edge behavior of the photocurrent excitation spectra Eqs. (26), (36) are opposite to the electron case. The reason is in the complicated valence band structure. For example, the parabolic behavior (26) contrasts to the electron one Eq. (19) due to the k^2 -dependence of the tensor β_{BIA} for holes, Eq. (23).

V. RESULTS AND DISCUSSION

Equations (13) - (18), (23) - (25), and (31) - (35) describe the contributions to the circular photocurrent due to interband optical transitions. It is seen that the symmetry of the system determines the direction of the current. Indeed, according to Eq. (14), $j_i(\omega) \propto \beta_{li} \hat{o}_l$, i.e. (i) the current appears only under oblique light incidence in (001)-grown QWs, and (ii) for SIA the current \mathbf{j} is perpendicular to \hat{o} , while for BIA the angle between \mathbf{j} and \hat{o} is twice larger than the angle between the axis [100] and \hat{o} , see Fig. 1.

The spectrum of the photocurrent is determined by the functions $G(k_\omega)$. Figure 2 presents the partial contributions to this function for both SIA and BIA electron spin splittings calculated for a 100-Å wide QW with infinitely-high barriers. The interband transitions from the $h1$, $h2$, $l1$ and $h3$ hole subbands to the ground electron subband $e1$ are taken into account. The effective masses of the electron, heavy- and light-holes are chosen to correspond to GaAs: $m_e = 0.067m_0$, $m_{hh} = 0.51m_0$, $m_{lh} = 0.082m_0$. The momentum relaxation times are assumed to be related by $\tau_h = 2\tau_e$ and independent of the carrier energies.³⁶

The edge behavior of the photocurrent is due to the $h1 \rightarrow e1$ transitions. One can see the linear and quadratic raising of the current near the absorption edge in accordance with Eq. (19). At higher energies, the spectra are determined mainly by the $h1 \rightarrow e1$ and $h2 \rightarrow e1$ transitions. The difference between BIA and SIA spectra is crucial: although in both cases the current for the $h2 \rightarrow e1$ transitions is mainly negative and has a minimum, in the BIA-induced photocurrent these transitions give twice smaller contribution than $h1 \rightarrow e1$, while for SIA-dominance they give the main contribution.

The total circular photocurrent caused by the four kinds of optical transitions is presented in Fig. 3. The arrows in Fig. 3 indicate the points where the transitions start. One can see that the BIA-induced circular photocurrent has a peak in the spectrum, while in the SIA case the dip is present around the same point. This photon energy corresponds to excitation of carriers with $k \approx 2/a$, where a is the quantum well width. At this point the $h1$ and $h2$ energy dispersions have an anti-crossing. This results in a transformation of the hole wave functions and, hence, substantial changes in the dependence $G(k)$.

The main feature of Fig. 3 is that the BIA-photocurrent has no sign change in the given energy domain, while in the SIA-case it has a sign-variable spectrum. This makes possible to determine the structure symmetry by means of the photogalvanic measurements.

VI. CONCLUDING REMARKS

The situations are possible when the both SIA and BIA are present. The absolute value of the current in the case

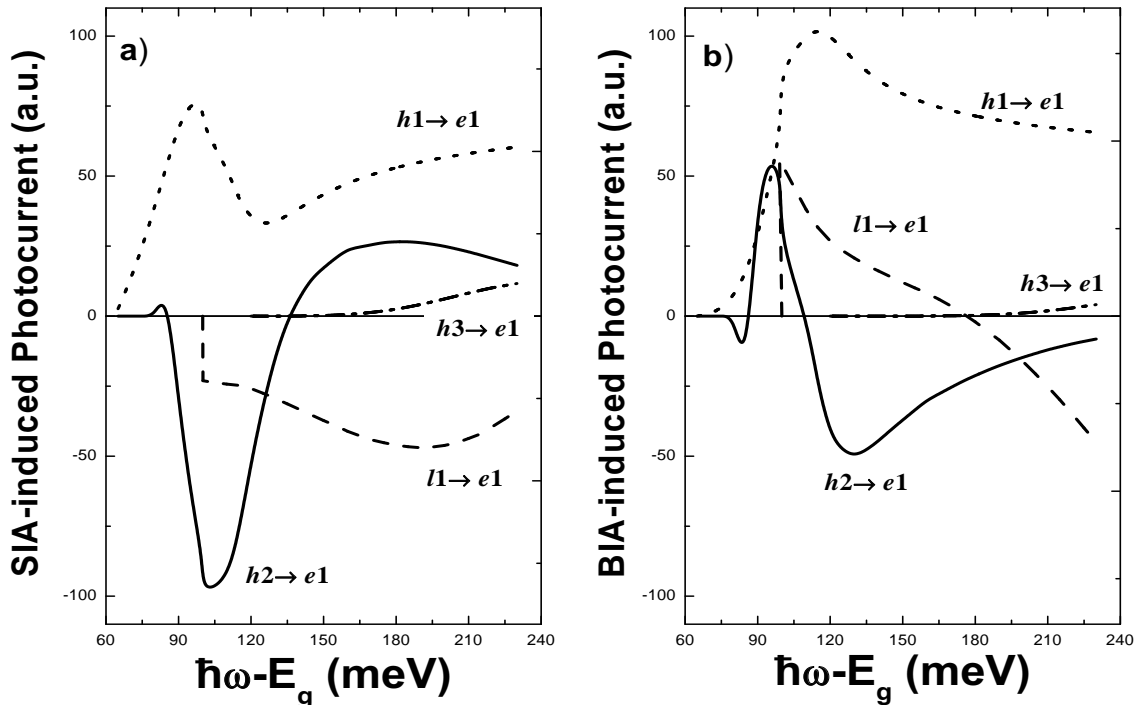


FIG. 2: Partial contributions to the circular photocurrent for direct interband transitions. Spin splitting of the electron states is due to SIA (a) or BIA (b).

$\beta_{\text{SIA}} \cdot \beta_{\text{BIA}} \neq 0$ is given by

$$j(\omega) = \sqrt{j_{\text{BIA}}^2(\omega) + j_{\text{SIA}}^2(\omega) \mp 2j_{\text{BIA}}(\omega)j_{\text{SIA}}(\omega) \sin 2\phi}, \quad (37)$$

where ϕ is the angle between \hat{o} and the axis [100]. The upper (lower) sign in Eq. (37) corresponds to $\beta_{\text{BIA}} \cdot \beta_{\text{SIA}} > 0$ (< 0). The direction of the photocurrent is given by the angle ψ between $[1\bar{1}0]$ and \mathbf{j} :

$$\tan \psi = \frac{j_{\text{SIA}}(\omega) + j_{\text{BIA}}(\omega)}{j_{\text{SIA}}(\omega) - j_{\text{BIA}}(\omega)} \tan(\phi - \pi/4). \quad (38)$$

The angular dependence (37) occurs due to simultaneous presence of Rashba and Dresselhaus fields ($\beta_{\text{SIA}} \cdot \beta_{\text{BIA}} \neq 0$) by analogy with the $\phi_{\mathbf{k}}$ -dependence of the spin splitting. It should be noted that j_{SIA} and j_{BIA} have different excitation spectra that causes complicated ω -dependences of the total photocurrent absolute value and direction, Eqs. (37), (38).

The analysis shows that, under anisotropic scattering, the “interference” terms $\beta_{\text{BIA}} \cdot \beta_{\text{SIA}} / (\beta_{\text{BIA}}^2 + \beta_{\text{SIA}}^2)$ appear in the total photocurrent Eq. (13) even in the linear in

β 's regime. This is caused by coupling of the Fourier harmonics of the velocity operator and density matrix in Eq. (5).

In conclusion, we have developed a theory of the interband circular photogalvanic effect in QWs. The cases when either SIA, BIA or IIA dominates have been considered. It is shown that SIA and BIA result in non-equal photocurrents in QWs. Their excitation spectra have absolutely different shapes in the whole studied range. This makes the interband circular photogalvanic effect a unique highly sensitive tool for investigation of symmetry and spin properties of QWs.

Acknowledgments

The author thanks E.L. Ivchenko for helpful discussions and S.D. Ganichev for a critical reading of the manuscript. This work was financially supported by the RFBR, DFG, INTAS, “Dynasty” Foundation — ICFPM, and by the Programmes of RAS and Russian Ministries of Science and Education.

* Electronic address: golub@coherent.ioffe.ru

¹ *Semiconductor Spintronics and Quantum Computation*, edited by D.D. Awschalom, D.Loss, and N. Samarth,

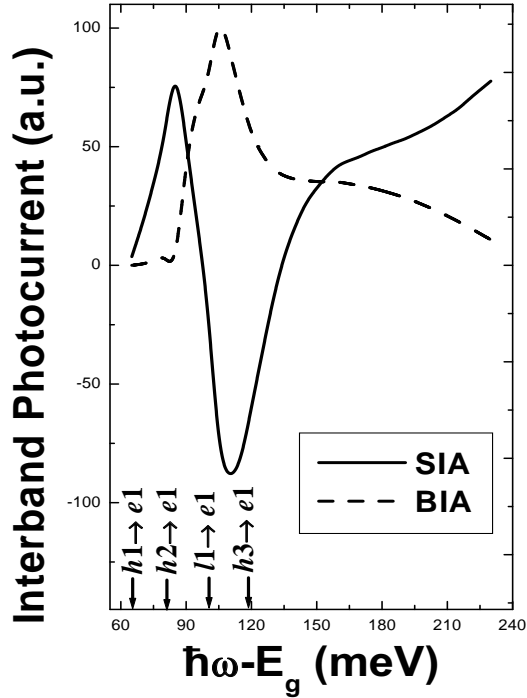


FIG. 3: Spectrum of the interband circular photocurrent due to SIA (solid line) and BIA (dashed line) electron spin splittings in a 100-Å wide QW. The arrows indicate the absorption edges for the four optical transitions.

(Springer, Berlin, 2002).

- ² S. Datta and B. Das, *Appl. Phys. Lett.* **56**, 665 (1990).
- ³ Y.A. Bychkov and E.I. Rashba, *Pis'ma ZhETF* **39**, 66 (1984) [*JETP Lett.* **39**, 78 (1984)].
- ⁴ M.I. D'yakonov and V.Yu. Kachorovskii, *Fiz. Tekh. Poluprov.* **20**, 178 (1986) [*Sov. Phys. Semicond.* **20**, 110 (1986)].
- ⁵ E. A. de Andrada e Silva, *Phys. Rev. B* **46**, 1921 (1992).
- ⁶ F.G. Pikus and G.E. Pikus, *Phys. Rev. B* **51**, 16928 (1995).
- ⁷ W. Knap, C. Skierbiszewski, A. Zduniak, E. Litvin-Staszewska, D. Bertho, F. Kobbi, J.L. Robert, G.E. Pikus, F.G. Pikus, S.V. Iordanskii, V. Mosser, K. Zekentes, and Yu.B. Lyanda-Geller, *Phys. Rev. B* **53**, 3912 (1996).
- ⁸ P. Pfeffer and W. Zawadzki, *Phys. Rev. B* **52**, R5312 (1999).
- ⁹ N.S. Averkiev and L.E. Golub, *Phys. Rev. B* **60**, 15582 (1999).
- ¹⁰ Y.-C. Chang and J. N. Schulman, *Phys. Rev. B* **31**, 2056 (1985); **31**, 2069 (1985).
- ¹¹ I. L. Aleiner and E. L. Ivchenko, *Pis'ma Zh. Eksp. Teor. Fiz.* **55**, 662 (1992) [*JETP Lett.* **55**, 692 (1992)].
- ¹² E. L. Ivchenko, A. Yu. Kaminski, and I. L. Aleiner, *Zh. Eksp. Teor. Fiz.* **104**, 3401 (1993) [*JETP* **77**, 609 (1993)].
- ¹³ E. L. Ivchenko, A. Yu. Kaminski, and U. Rössler, *Phys. Rev. B* **54**, 5852 (1996).
- ¹⁴ O. Krebs and P. Voisin, *Phys. Rev. Lett.* **77**, 1829 (1996).
- ¹⁵ O. Krebs, D. Rondi, J. L. Gentner, L. Goldstein, and P. Voisin, *Phys. Rev. Lett.* **80**, 5770 (1998).
- ¹⁶ B. Foreman, *Phys. Rev. Lett.* **86**, 2641 (2001)
- ¹⁷ S. Cortez, O. Krebs, and P. Voisin, *J. Vac. Sci. Technol. B* **18**, 2232 (2000); *Eur. Phys. J. B* **21**, 241 (2001).
- ¹⁸ L. Vervoort, R. Ferreira, and P. Voisin, *Phys. Rev. B* **56**, R12744 (1997).
- ¹⁹ T. Guettler, A. Triques, L. Vervoort, R. Ferreira, Ph. Rousignol, P. Voisin, D. Rondi and J.C. Harmand, *Phys. Rev. B* **58**, R10179 (1998).
- ²⁰ L. Vervoort, R. Ferreira, and P. Voisin, *Semicond. Sci. Technol.* **14**, 227 (1999).
- ²¹ U. Rössler and J. Kainz, *Solid State Commun.* **121**, 313 (2002).
- ²² D. Stein, K. von Klitzing, and G. Weimann, *Phys. Rev. Lett.* **51**, 130 (1983).
- ²³ B. Jusserand, D. Richards, G. Allan, C. Priester, and B. Etienne, *Phys. Rev. B* **51**, 4707 (1995).
- ²⁴ P. D. Dresselhaus, C. M. A. Papavassiliou, R. G. Wheeler, and R. N. Sacks, *Phys. Rev. Lett.* **68**, 106 (1992).
- ²⁵ N. S. Averkiev, L. E. Golub and M. Willander, *J. Phys.: Condens. Matter* **14**, R271 (2002).
- ²⁶ E.L. Ivchenko, and G.E. Pikus, *Superlattices and Other Heterostructures. Symmetry and Optical Phenomena*, (Springer, Berlin, 1997).
- ²⁷ S.D. Ganichev, E.L. Ivchenko, S.N. Danilov, J. Eroms, W. Wegscheider, D. Weiss, and W. Prettl, *Phys. Rev. Lett.* **86**, 4358 (2001).
- ²⁸ S.D. Ganichev E.L. Ivchenko, V.V. Bel'kov, S.A. Tarasenko, W. Wegscheider, D. Weiss, and W. Prettl, *Nature (London)* **417**, 153 (2002).
- ²⁹ I.A. Merkulov, V.I. Perel', and M.E. Portnoi, *Zh. Eksp. Teor. Fiz.* **99**, 1202 (1991) [*Sov. Phys. JETP* **72**, 669 (1991)].
- ³⁰ Expressions for the real coefficients N , W_{\pm} , Q_{\pm} , and for the functions $\chi_{\pm}(z)$ are given in Ref. 29 in the approximation of infinitely-high barriers.
- ³¹ E.L. Ivchenko, Yu.B. Lyanda-Geller and G.E. Pikus, *Zh. Eksp. Teor. Fiz.* **98**, 989 (1990) [*Sov. Phys. JETP* **71**, 550 (1990)].
- ³² R. Winkler, *Phys. Rev. B* **62**, 4245 (2000).
- ³³ S.D. Ganichev, U. Rössler, W. Prettl, E.L. Ivchenko, V.V. Bel'kov, R. Neumann, K. Brunner, and G. Abstreiter, *Phys. Rev. B* **66**, 75328 (2002).
- ³⁴ S.D. Ganichev, E.L. Ivchenko, and W. Prettl, *Physica E* **14**, 166 (2002).
- ³⁵ see also O. Mauritz and U. Ekenberg, *Phys. Rev. B* **55**, 10729 (1997).
- ³⁶ The contribution of the only "allowed" transition $l1 \rightarrow e1$ is proportional to $(\tau_h - \tau_e)$ at $k = 0$, therefore we take different values for τ_e and τ_h in order to obtain a step-like behavior of the spectrum. It is clearly seen in the corresponding curves in Figs. 2(a) and 2(b).